Journal of Applied Electrochemistry **34**: 37–46, 2004.

Electrochemical behaviour of galena (PbS) in aqueous nitric acid and perchloric acid solutions

Yu. MIKHLIN[1,*], A. KUKLINSKIY[1], E. MIKHLINA[1], V. KARGIN[1] and I. ASANOV[2]
[1]*Institute of Chemistry and Chemical Technology of SB RAS, Krasnoyarsk, 660049, Russia*
[2]*Institute of Inorganic Chemistry of SB RAS, Novosibirsk, 630090, Russia*
*(*author for correspondence, fax: +7 3912 238658, e-mail: yumikh@icct.ru)*

Received 26 February 2002; accepted in revised form 9 May 2003

Key words: disordered semiconductor, lead sulfide, nitric acid, perchloric acid, sulfuric acid, voltammetry, XPS

Abstract

The electrochemical reactions of natural n-type PbS in nitric and perchloric acid solutions have been studied using cyclic voltammetry, SEM and XPS. Several oxidation stages, which differ in their electrode kinetics, surface topography and sulfide phase composition, particularly Pb/S ratios and the state of sulfur, were demonstrated. The quantities of surface sulfate and thiosulfate were rather low at PbS oxidized in HNO_3 solutions, even at high potentials. The magnitude of the reoxidation peaks of cathodically formed products, primarily Pb^0, was found to increase as the electrodissolution of PbS on the preliminary positive-going sweep was hindered. It is proposed that the predominant donor-like defects in the disordered reaction layers limit the concentration and mobility of holes, thus inhibiting PbS oxidation and promoting metallic lead deposition in the course of potential cycling. The model developed as an alternative to the traditional explanations uses the concept of negative correlation energy centres resembling those in non-crystalline chalcogenide semiconductors.

1. Introduction

Lead sulfide is of importance both as the principal mineral of lead (galena) and a material for optoelectronics. Although its electrochemistry and surface chemistry have received much attention, basic features of the PbS electrochemical behaviour are still not understood. The rates of anodic oxidation of PbS vary considerably in different solutions in spite of the fact that elemental sulfur is the main oxidation product

$$PbS \rightarrow Pb^{2+} + S^0 + 2e^- \quad (1)$$

while the cathodic curves are fairly similar [1–10]. Paul and coworkers [1, 2] studied galena electrochemistry in perchlorate and sulfate media by the rotating ring-disk technique and showed that the voltammetric curves display a first anodic maximum or shoulder at a potential of 0.3–0.5 V vs SCE and a principal peak at higher biases. It is interesting that the small anodic maximum at 0.3 V in sulfuric acid coincided with a sudden peak of the ring current of Pb^{2+} reduction that was normally small owing to the low solubility of $PbSO_4$. The effect of illumination on the anodic dissolution, which means that the surface density of holes partly limits the PbS oxidation rate, disappeared at potentials higher than 0.4 V [1, 7]. The first maximum was ascribed to Reaction 1 which proceeds at certain 'active' surface sites and produces a layer of sulfur covering these sites, and the main peak was related to the formation of a passive film of basic lead sulfates [1]. The morphology of the anodically produced sulfur was thought to have a bearing on the behaviour of galena [1–4, 10]. Recently Nava et al. [10] assumed that elemental sulfur inhibits the electrodissolution of galena in perchlorate media (pH 0), with aqueous Pb^{2+} ions imparting a greater porosity to the film of S^0. In hydrochloric acid solutions, three anodic maxima, with the most intensive one at about 0.4 V, were usually observed. Dandapani and Ghali [3] suggested that the passivation phenomena are due to successive formation of crystalline sulfur, lead chloride and lead sulfate

$$PbS + 4\,H_2O \rightarrow PbSO_4 + 8H^+ + 8e^- \quad (2)$$

On the other hand, the anodic oxidation of PbS in 1 M sulfuric acid was crucially dependent on small additions of different anions which did not effect $PbSO_4$ solubility [5]. It was proposed that the anionic composition of the electrolyte influences the rate of lead release and, hence, the formation of a non-equilibrium metal-deficient surface layer

$$PbS + L \rightarrow x\,Pb^{2+} + Pb_{1-x}S + L + 2xe^{-} \quad (3)$$

which is responsible for the metal sulfide passivation [5, 11–13].

Acidic nitrate solutions, being one of few media with high solubility of the lead salt, are promising for lead hydrometallurgy and for investigations of PbS electrochemistry fundamentals, but little research has been conducted in these electrolytes. Holmes and Crundwell [7] examined the anodic oxidation of PbS in a 0.5 M HNO_3 + 0.6 M $NaNO_3$ solution at potentials lower than 0.65 V vs SCE and found a shoulder at 0.48 V, which was ascribed to oxidation of the passive film of elemental sulfur. The anodic current was independent of the electrode rotation rate, the Tafel slopes varied from 75 to 130 mV decade^{-1} between potentials of 0.25 and 0.4 V, the apparent activation energy was 72 kJ mol^{-1} at 0.45 V, so the authors concluded that the oxidation rate was controlled by a surface reaction. Pashkov et al. [14] reported that the dissolution of galena in nitric acid solutions proceeded via the non-oxidative pathway producing H_2S at electrode potentials less than 0.1–0.2 V vs Ag/AgCl. At higher potentials, a rotating disk electrode of PbS dissolved for the most part anodically, showing in 1 M HNO_3 the highest rate at about 0.6 V.

It is known that semiconducting properties of thin films of A^2B^6 and A^4B^6 compounds alter irreversibly as a result of oxygen adsorption and initial stages of their oxidation, probably owing to diffusion of interstitial and then lattice cations to the surface, forming metal vacancies and a p-type surface layer [15–17]. The layers of sulfide reacted under severer conditions are more notably modified. Galena, oxidized in air or conditioned in liquids, was characterized by means of X-ray photoelectron spectroscopy (XPS) in a number of studies focussed largely on detection of oxygen-containing surface products [12, 13, 18–30]. An enrichment in sulfur over metal, often well beyond the stability range, was found for many reacted metal sulfides including PbS [12, 13, 18–21]. It was determined by XPS, UPS and X-ray spectroscopies that electronic band structures of, surprisingly, up to micrometres thick zones of PbS etched in acidic solutions are distorted by plentiful centres related to over-stoichiometric sulfur [26, 28], so the metal-deficient layers should be considered as disordered semiconductors similar to noncrystalline chalcogenides [31–34]. Structural changes and submicrometre scale nonhomogeneity of the reacted PbS surfaces were also detected using scanning probe microscopy (STM, STS, AFM) [20–23, 35–40].

In this work, the electrochemical reactions of natural lead sulfide in nitric and perchloric acid solutions were examined by cyclic voltammetry, the composition and morphology of the electrode surfaces were monitored using *ex situ* XPS and scanning electron microscopy (SEM). The purpose of the research was to gain further insight into the role of surface layer modifications in PbS oxidation kinetics. We put forward an unconventional reaction mechanism, which brings into consideration concepts developed in the physics of noncrystalline chalcogenide semiconductors.

2. Experimental details

Polycrystalline galena obtained from Geological Museum of Central Siberia (origin Taimyr, Russia) had less than 0.1% by mass of iron, zinc, copper and silver as the major impurities and no inclusions of other phases. The material was of n-type conductivity with $(3–9) \times 10^{17}$ cm^{-3} electron density determined from Hall effect measurements. Electrodes were cut from massive mineral specimens to obtain samples with approximately 4 mm × 5 mm × 5 mm edges. Copper was electrochemically deposited on the side opposite to a working surface of the sample, and then tinned copper wire was soldered to the Cu coating. The specimens were embedded in Teflon, with the working face of the electrode exposed. Before the experiments, fresh electrode surface was prepared by abrasion on silicon carbide paper, cleaning with filter paper and rinsing with doubly distilled water. After each experiment the used galena electrodes were repolished and reused. The experiments were performed with a potentiostat PI-50-1 equipped with a programmer PR-8 and an X–Y recorder. A three-compartment glass cell was used, and the counter and reference electrodes were platinum wire and saturated Ag/AgCl electrode, respectively. The potentials are quoted with respect to the latter. Solutions were prepared from reagent grade chemicals and doubly distilled water; argon was used to purge oxygen from solutions.

The experiments were conducted using a stationary electrode at 20 ± 1 °C, some tests were undertaken employing a RDE. The sweep rate was 5 mV s^{-1} unless otherwise stated. Several experiments were carried out with single crystals of galena (unknown origin), and only minor differences in behaviour of various samples were observed. For SEM experiments the potential of the PbS electrode was swept to a predetermined value. The electrode was removed from electrolyte, rinsed with water and transferred into a chamber of a REMMA-202M electron microscope. The electrode was in contact with air for 2–3 min. The XPS spectra were obtained from galena specimens without plastic coatings treated in the same way, using an X-ray photoelectron spectrometer VG Microtech with MgK_α (1253.6 eV) as a photon source at room temperature and a pressure of about 10^{-8} Pa. The analyser pass energy was 20 eV. Spectra from the abraded sample without polarization and the mineral ground to a particle size of approximately 70 μm were acquired for comparison. Binding energies (BE) were calculated using the C 1s peak (285.0 eV) as an internal reference. After subtracting a nonlinear background, each spectrum was resolved into individual component bands of a convoluted gaussian-lorentzian (50%) lineshape. Surface concentrations of

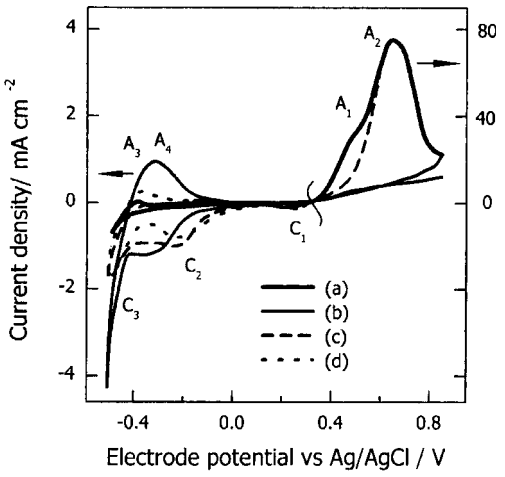

Fig. 1. Cyclic voltammograms of a stationary PbS electrode in 1 M HNO_3, scan rate 5 mV s^{-1}: (a) first scan was initiated in the negative-going direction, the limits of the positive-going sweep before the second scan were (b) 0.8, (c) 0.6 and (d) 0.4 V. Current density scales for left and right axes differ by a factor of 20.

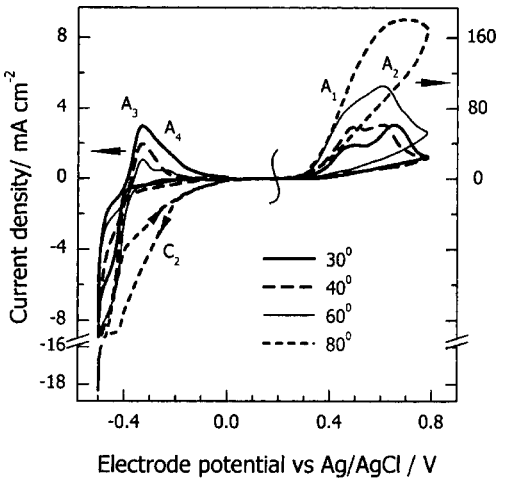

Fig. 2. Effect of temperature on voltammetry of PbS in 1 M HNO_3. The sweep was initiated in the positive-going direction.

elements were determined from peak areas corrected for the photoionization cross sections [41].

3. Results

3.1. *Voltammetry*

Typical cyclic voltammograms of the stationary lead sulfide electrode in 1 M HNO_3 are shown in Figure 1. A shoulder A_1 at a potential of about 0.5 V and a main peak A_2 centred at 0.65 V on the positive-going sweep are almost independent of stirring the electrolyte and the preliminary negative potential excursion, but they practically disappear in the second positive scan. After the oxidation, the cathodic currents in maxima C_1, C_2 and a surge C_3 are greater by a factor of about 5 than those on the sweep initiated first in the negative direction, but are by dozens of times less than the anodic ones, implying that only a minor part of the oxidation products undergoes the reduction. When the potential sweep is reversed from its most negative value of −0.5 V, an anodic maximum composed of two unresolved peaks A_3 and A_4 is observed at a potential of about −0.3 V. The feature magnitude is small if the sweep is started first in the negative direction and depends on the limit of the preliminary positive-going sweep: it increases when the limit is extended to 0.5 V, then diminishes after the excursion to 0.6 V, and grows considerably as the sweep passes the major anodic peak A_2. The charge associated with the maxima A_3–A_4 in the curve (b) amounts to 0.03 C cm^{-2}.

Tafel slopes were measured from the voltammetric curves in the range 0.2 to 0.35 V, where plots of log i against potential are roughly linear. The slopes are 110 ± 10 mV $decade^{-1}$, in agreement with those obtained by Holmes and Crundwell [7], suggesting an involvement of charge transfer into a rate-determining step. Potentiostatic current transients have complex shapes, usually displaying a fast decrease in initial 10–100 s and then two or three maxima during a 1 h experiment [14].

Figure 2 shows that the maximum A_1 increases more rapidly than A_2 with increase in temperature. Apparent activation energies, E_A, determined for chronoamperometric plots under potentiostatic conditions are found to be time- and potential-dependent. E_A of 22 kJ mol^{-1} is comparably stable at 0.4 V; it decreases from 29 kJ mol^{-1} for 100 s to 23 kJ mol^{-1} for 600 s at 0.5 V, from 24 to 14 kJ mol^{-1} at 0.6 V, and from 46 to 29 kJ mol^{-1} at 0.7 V. These data suggest transport control or mixed transport-kinetic control of the oxidation process, seemingly contradicting the voltammetric results as the lower E_A meanings are related to the 'active' anodic dissolution (0.4 and 0.6 V), whereas the higher E_A pertains to the 'passive' region above 0.65 V.

As nitric acid concentration increases from 0.1 to 2 M, the peak A_2 shifts to less positive potentials, having a maximal height in 0.5–1.0 M HNO_3, while the shoulder A_1 increases steadily, as well as the peak A_3 does

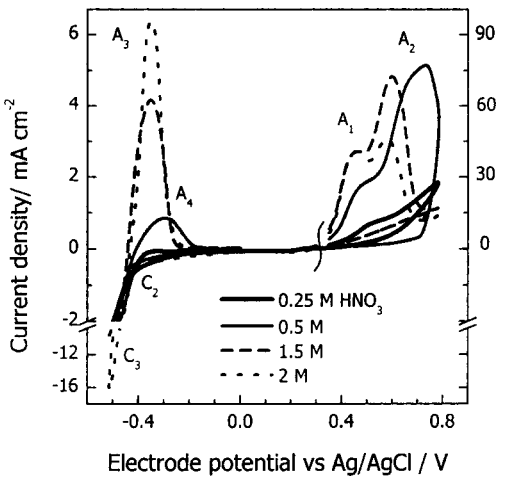

Fig. 3. Effect of nitric acid concentration on voltammograms of PbS. Sweep initiated in positive-going direction.

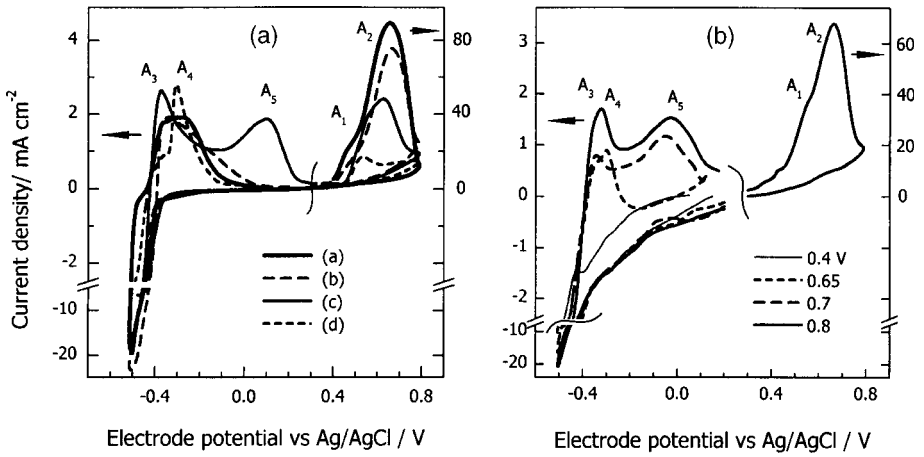

Fig. 4. Voltammograms of PbS in mixtures of nitric and sulfuric acid. A: (a) 0.99 M HNO_3 + 0.01 M H_2SO_4, (b) 0.95 M HNO_3 + 0.05 M H_2SO_4, (c) 0.75 M HNO_3 + 0.25 M H_2SO_4, (d) 0.5 M HNO_3 + 0.5 M H_2SO_4. B: 0.9 M HNO_3 + 0.1 M H_2SO_4; numbers near cathodic curves stand for limits of the preliminary positive sweep.

(Figure 3). Additions of KNO_3 to 0.1 M HNO_3 accelerate the oxidation, although it remains somewhat slower in 0.9 M KNO_3 + 0.1 M HNO_3 than in 1 M HNO_3. The anodic process is, therefore, affected chiefly by the anion concentration, but the acidity also plays a role.

Experiments carried out in mixtures of nitric and sulfuric acids (Figure 4) demonstrate that the oxidation slows down gradually with increase in H_2SO_4 concentration, when the concentration is above 0.01 M. In media containing 0.1–0.25 M H_2SO_4, the peaks A_3 and A_4 enhance notably; extending the positive sweep to 0.7 V or higher causes a new broad peak A_5 at −0.05–+0.1 V (Figure 4B). Additions of chloride-ions (not presented in Figures) also impede the anodic oxidation in nitric acid solutions and promote processes in the features A_3, A_4 and A_5.

The maxima A_3, A_4 and A_5 were usually considered to correspond to a reaction of metallic lead with hydrogen sulfide forming PbS, oxidation of lead to Pb^{2+}

$$Pb^0 \rightarrow Pb^{2+} + 2e^- \qquad (4)$$

and oxidation of hydrogen sulfide to S^0, respectively [2–4, 6]. Metallic lead is known to deposit from an electrolyte at about −0.4 V, and PbS decomposes producing Pb^0 and H_2S at potentials lower than −0.5 V [2, 4]. Scott and Nicol [42] and recently Cisneros-Gonzalez et al. [8,9] performed voltammetric studies in this potential region in 0.5 M HCl and in a NaCl solution having pH 2 and also ascribed the maximum A_5 to Reaction 4. Moreover, very similar three-peak patterns were observed for lead deposited on gold electrodes [43,44] and were assigned to Pb^0 oxidation at different surface sites. In the presence of aqueous lead nitrate, a considerable enlargement of peak A_3 at −0.38 V (Figure 5) is observed. This appears to originate from the bulk metal oxidation, whereas the maxima A_4 and A_5 are attributable to the reaction of Pb^0 deposited at different PbS areas.

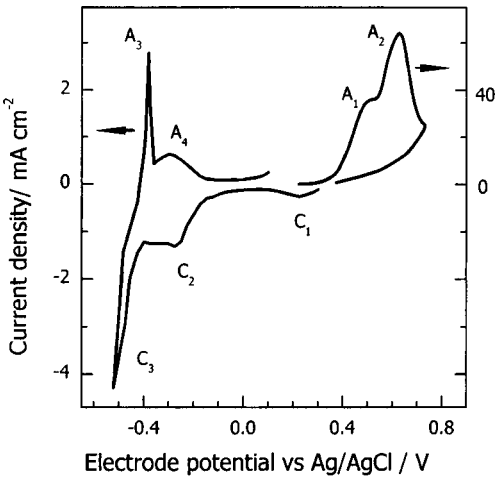

Fig. 5. Cyclic voltammogram of PbS in 1 M HNO_3 + 0.01 M $Pb(NO_3)_2$ electrolyte. Sweep initiated in positive-going direction.

A small shoulder at approximately 0.45 V and a broad peak at about 1 V occur in the positive-going potential sweep in 1 M $HClO_4$ (Figure 6). The peak magnitude is close to that in 1 M HNO_3 solution and is almost insensitive to added extraneous anions; only small A_3 and A_4 peaks are observed at negative potentials. In pure sulfuric acid solutions, the anodic current in the main maximum centred at about 0.8 V is less than in nitrate and perchlorate media (Figure 6, see also [1, 3, 5]), but it exceeds the currents of PbS oxidation in hydrochloric acid electrolytes. The peak is reproduced on the negative-going scan; maxima A_3, A_4, A_5 are absent. These facts signify that the thick lead sulfate coating formed in solutions containing high concentrations of sulfate-ions neither irreversibly screens the PbS surface, nor facilitates Pb^{2+}/Pb^0 conversion. In our opinion, the effects of acid anions and ligand additions can not be rationalized in terms of the formation of insoluble lead salts or/and elemental sulfur, which would block the PbS dissolution. The

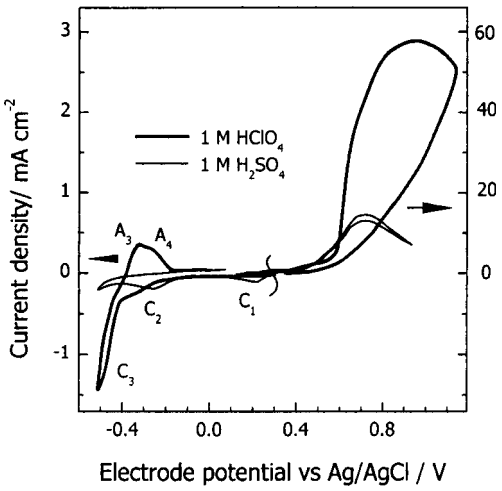

Fig. 6. Voltammograms of PbS in 1 M $HClO_4$ and 1 M H_2SO_4. Sweep initiated in positive-going direction.

affinity of the passive surfaces to metallic lead also needs to be clarified.

3.2. *Scanning electron microscopy*

Secondary electron micrographs of the PbS surfaces (formed mainly by (100) faces) polarized in 1 M HNO_3 to various potentials are given in Figure 7 (the charge densities passed are presented in Table 1). Small amounts of non-uniformly allocated products and etching pits of 100–500 nm in diameter are barely perceptible for the sweep limit of 0.4 V; the pits become abundant and start to evolve into a cross configuration at 0.5 V (Figure 7(a)). After potential scanning extending to 0.6 and 0.7 V, the surface is covered with narrow intersected pits less than 500 nm wide and 1000–5000 nm in length, parallel to the ⟨010⟩ and equivalent orthogonal direction, and with rounded cavities. The formation of the etching pits oriented in certain crystalline lattice directions infers that the dissolution is controlled, fully or partially, by a solid-state reaction, probably incongruent, because square pits but not elongated ones would arise due to a successive extraction of Pb and S atoms from the (100) surface of NaCl-type cubic crystals [45]. It is worth noting that, according to the STM data, the aerial oxidation [35], initial dissolution, and cathodic reduction of PbS to Pb [39] occur preferentially along the ⟨010⟩ directions. For the sweep limit of 0.8 V, the products cover a large part of the surface, and rounded pits up to 1000 nm in diameter develop instead of the elongated pits (Figure 7(c)). Residual fragments of the structure obtained at less positive potentials are observed in some spots (Figure 7(d)). In 1 M $HClO_4$, the surface with cross and round etching pits remains stable at 1.0 V (Figure 8) when the anodic current is high.

3.3. *XPS characterization*

The spectra obtained from PbS samples oxidized in 1 M HNO_3 solution in the positive-going scan to 0.4 and 0.6 V do not show appreciable quantities of lead sulfate and elemental sulfur, which is known to be volatile in the ultrahigh vacuum at ambient temperature [18, 25], but a small amount of oxysulfur species occurs on the surface polarized in the scan to 0.5 and 0.8 V (Figure 9). The principal S 2p bands are shifted by 0.4–0.6 eV to higher BE, probably due to a change in the local charge of S atoms in the anionic sublattice or/and a variation of the Fermi level position with respect to the band edges [26]. In each case, the band can be resolved into two

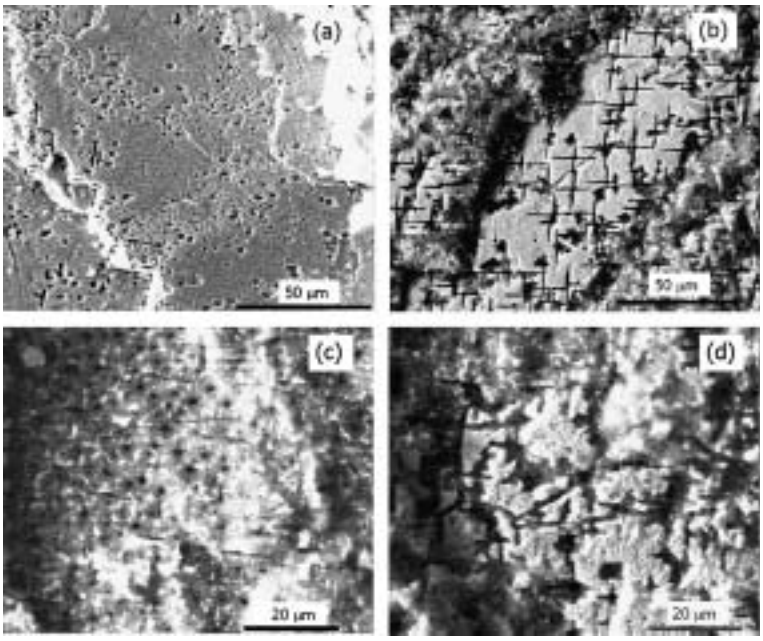

Fig. 7. SEM images of PbS electrodes oxidized in 1 M HNO_3 in the anodic sweep to (a) 0.5, (b) 0.7 and (c and d) 0.8 V.

Table 1. XPS parameters for PbS anodized (scan rate 5 mV s^{-1}) in 1 M HNO_3

Sample treatment (charge passed)	Pb $4f_{7/2}$		S 2p		O 1s		Atomic ratios	
	BE /eV	*I* (%)	*BE* /eV	*I* (%)	*BE* /eV	*I* (%)	Pb/S*	Pb/O
Abraded in air	137.2	95	161.1	88	530.8	11	1.05	1.39
	138.2	5	161.7	12	531.6	24	(1.0)	
					532.5	38		
					533.5	27		
Polarized to 0.4 V	138.1	71	161.2	90	530.9	2	1.49	0.54
(0.079 C cm^{-2})	139.1	16	162.7	10	531.7	22	(1.06)	
	139.8	13			532.6	35		
					533.5	41		
Polarized to 0.5 V	138.2	74	161.2	76	531.7	25	1.09	0.59
(0.54 C cm^{-2})	139.1	18	162.6	10	532.7	36	(0.81)	
	139.8	8	166.9	14	533.7	39		
Polarized to 0.6 V	137.9	74	160.9	84	530.5	18	1.43	0.51
(1.36 C cm^{-2})	138.9	18	161.4	16	531.5	24	(1.06)	
	139.7	8			532.5	40		
					533.4	18		
Polarized to 0.8 V	137.6	82	160.8	56	531.4	17	0.81	0.50
(3.8 C cm^{-2})	138.7	13	162.0	8	532.4	29	(0.8)	
	139.5	5	163.1	20	533.3	33		
			165.2	10	534.3	13		
			167.8	6	535.1	8		

* Figures in parentheses correspond to sulfide phases.

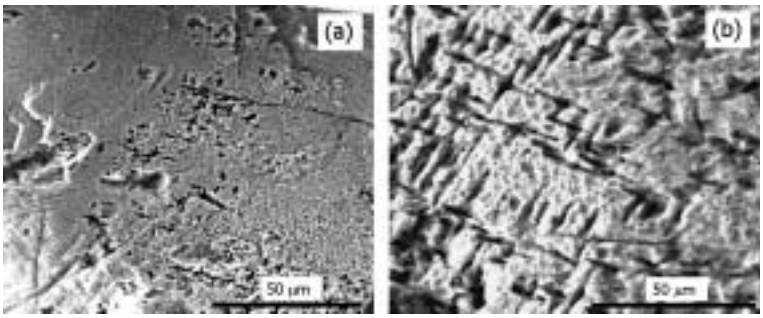

Fig. 8. SEM images of PbS electrodes oxidized in 1 M $HClO_4$ in the anodic sweep to (a) 0.6 and (b) 0.8 V.

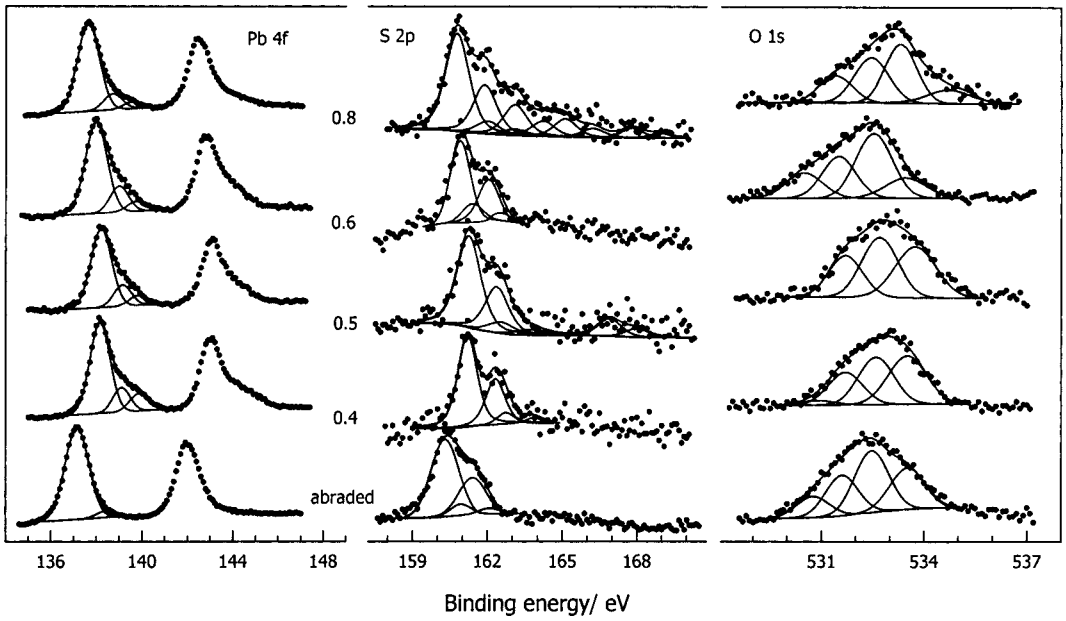

Fig. 9. X-ray photoelectron spectra of PbS samples abraded in air and oxidized in 1 M HNO_3 in the sweep to various potentials. Numbers near the spectra stand for the potential sweep limits.

doublets differing in their binding energies by 0.5–0.6 eV or about 1.5 eV. This may be related to surface nonhomogeneity, although the components at 162–162.7 eV may be attributable to disulfide species. The positive-going scan to 0.8 V gives rise to contributions at BE ~163.1 eV, ~165.2 eV and 167.8 eV. The intensity of the last line corresponding to thiosulfate is less than that at 163.1 eV, which, therefore, is only partly due to $S_2O_3^{2-}$ but mainly to polysulfide species. The Pb 4f spectrum becomes asymmetrical after electrochemical oxidation, with weaker components on its high BE side associated with lead oxide/hydroxide, nitrate and oxysulfur salts. These species could be precipitated owing to rinsing the electrode with water, entrapped in the surface topography heterogeneities, or formed as a consequence of PbS_xO_y decomposition [29, 30]. The O 1s spectra contain contributions from O^{2-} (~530.5 eV) and OH^- (~531.5 eV) species, chemically (~532.5 eV) and physically (~533.5 eV) attached water.

A lead deficiency at the sulfide surfaces seems to arise as the potential is shifted from 0.4 to 0.5 V, to disappear at 0.6 V, and to develop again as the positive-going sweep reaches 0.8 V. The Pb/S ratios are calculated to be 1.06, 0.8, 1.06 and 0.8, respectively (Table 1), indicating two formation and decomposition cycles of the metal-deficient layer of PbS over the sweep; those are also seen in the SEM images. The differences between these values exceed the experimental error estimated as ± 0.1, so they appear to reflect the real regularity, despite an ambiguity arising from the surface non-uniformity.

The XPS experiments performed with samples anodised in 1 M $HClO_4$ (Figure 10) show that the intensities of minor Pb $4f_{7/2}$ components at 139.0 and 139.6 eV are substantially increased. The last component is due to lead connected with ClO_4^-. This is consistent with the presence of Cl 2p line at 209.1 eV (Table 2); the strongest O 1s peak at BE of 533.6 eV also corresponds to perchlorate. The Pb/S ratios increase after the electrochemical oxidation, but the values for sulfide phase calculated by subtracting the oxidized lead concentrations are close to that for unreacted PbS. The S 2p spectra exhibit considerable lines shifted to higher BE by about 1.2 and 2.5 eV, which may be assigned to disulfide and polysulfide species, although it is unclear how S-S bonding takes place in the surface layer with minor or no excess of sulfur. In addition to the S 2p spectra, S 2s spectra were acquired (about 30 min later) in order to eliminate interfering effects of the Pb 4f energy loss maxima, which overlap the S 2p bands. Qualitatively, both sulfur lines show the same features (Table 2), but an obvious discrepancy occurs for the sample treated in the potential scan to 0.8 V. These phenomena may be associated with partial decomposition or transformation of the unstable metal-depleted surface layer caused by radiation damage or other post-polarization effects rather than with a small difference in the photoelectron escape depths [41]. In particular, Buckley and Woods [13] pointed out a relaxation of the previously anodised, metal-deficient PbS surface at open circuit and under cathodic polarization that was suggested to be due to the solid-state diffusion of lead to the surface.

4. Discussion

The conventional approaches [1, 3, 6–10] suggest that different stages of lead sulfide oxidation are due to passivation of PbS by elemental sulfur, thiosulfate, sulfate, other salts or oxyhydroxides of lead. However, elemental sulfur is known to be rather stable and to oxidize very slowly even in nitric acid at elevated temperatures [46]. The high apparent activation energies in the passivity regions, the effect of anions and a

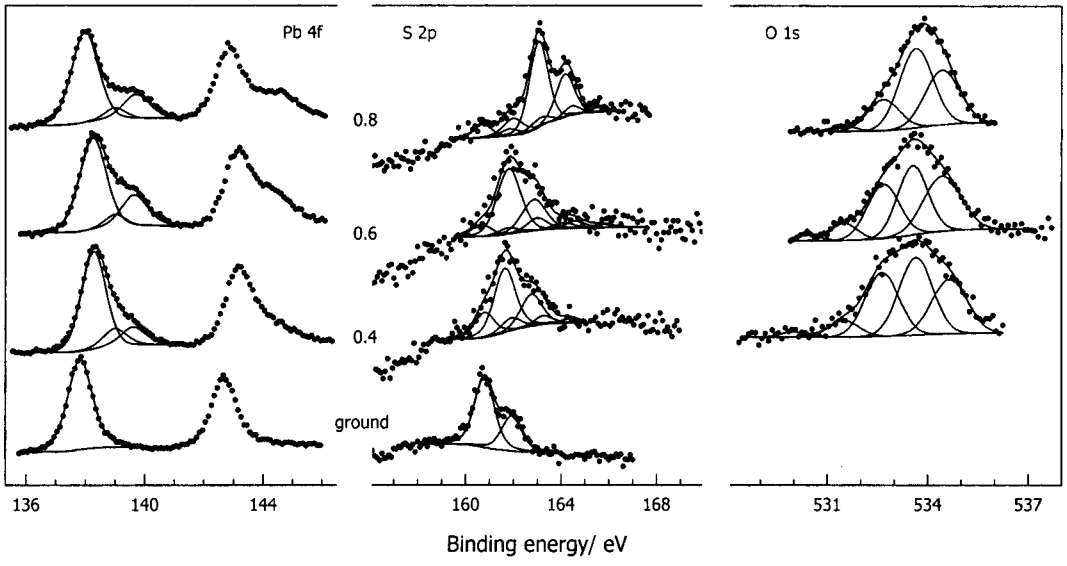

Fig. 10. X-ray photoelectron spectra of PbS samples ground in air and oxidized in 1 M $HClO_4$ in the anodic sweep to various potentials. Numbers near the spectra stand for the potential sweep limits.

Table 2. XPS parameters for PbS anodized (scan rate 5 mV s^{-1}) in 1 M $HClO_4$

Sample treatment (charged passed)	Pb $4f_{7/2}$		S 2p		S 2s		O 1s		Atomic ratios		
	BE /eV	*I* /%	*BE* /eV	*I* /%	*BE* /eV	*I* /%	*BE* /eV	*I* /%	Pb/S*	Pb/O	Pb/Cl
Air ground	137.8	100	160.8	100	225.6	90	–	–	1.4	–	–
					227.9	10			(1.09)		
Polarized to	138.3	71	160.8	25	225.7	15	530.0	2	2.0	2.4	–
0.4 V (0.017 C cm^2)	139.0	12	161.6	67	226.9	55	531.5	7	(1.3)		
	139.6	17	163.2	8	228.1	22	532.6	29			
					229.3	8	533.6	36			
							534.6	26			
Polarized to	138.3	67	160.7	11	225.6	16	530.4	2	1.8	3.0	4.2
0.6 V (0.14 C cm^2)	139.0	9	161.8	70	226.8	56	531.5	7	(1.4)		
	139.6	24	163.0	12	228.1	21	532.7	27			
			164.6	7	229.6	9	533.6	32			
							534.4	32			
Polarized to	138.0	70	160.7	11	225.6	11	531.5	2	1.9	2.9	1.9
0.8 V (1.68 C cm^2)	139.0	9	162.0	15	227.0	54	532.7	18	(1.5)		
	139.7	21	163.1	68	228.2	20	533.7	47			
			164.4	6	229.6	15	534.4	33			

* Calculated using S 2s spectra, figures in parenthesis are obtained using S 2p spectra.

relationship between the passivation and the peaks A_3, A_4, A_5 also remain unexplained. Alternatively, electrochemical kinetics may be associated with changes in the composition and structure of PbS surfaces, which were observed using XPS and SEM, although the results do not directly support an assumption [5, 11–13, 28] that the metal-deficient layers are responsible for passivation.

It is interesting that the deposition and following oxidation of metallic lead proceed on 'passive' surfaces, whereas the surfaces promoting the oxidation of PbS are almost inactive in respect to the Pb^{2+}/Pb^0 redox reactions. This would be explained by an increase in the near-surface concentration of lead ions because of their slow diffusion through a passive film to the solution, but large quantities of oxidized Pb species were also found by XPS at active surfaces. On the other hand, one can expect that Pb^0 forms easily on an n-type surface, while the anodic dissolution is facilitated by p-type conductivity of the semiconductor. The n to p-type conversion occurs during the initial stages of galena oxidation [16, 17], but the situation with distorted PbS structures is more complex. It is known that heavily doped crystalline semiconductors differ in many ways from their counterparts containing lesser quantity of defects. Furthermore, strong deformations of chemical bonds suggest that the reacted layers are essentially disordered and possibly amorphous (also [26]). The basic features of a disordered solid are violations of an intrinsic symmetry, enhanced mobility of atoms, electron correlation and localization effects [31, 34]. The properties of disordered and noncrystalline chalcogens and chalcogenides [31–34] are largely determined by the defect centres D^+/D^- with negative correlation energy (valence alternation pairs), which are associated with lone pair p-orbitals of under- and over-coordinated chalcogenide atoms. The accurate nature of the defects is, however, still disputable. The scheme of charging of the negative correlation energy centres (Figure 11(a)) was described in detail [31, 34]. In brief, an energy E is required to fill an empty orbital of the donor-like centre D^+, exhibiting an energy level A^+ in processes which are notably faster than the following atomic rearrangements. For slower electron transitions the value E is diminished by an energy W^+ of the conjoined conversion of chemical bonds involved in these centres, showing a level B^+. The capture of the second electron

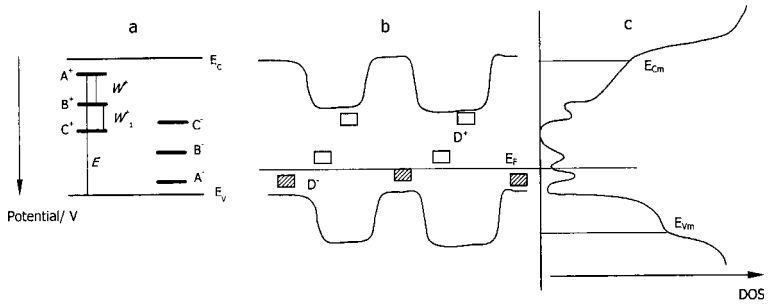

Fig. 11. Energy diagram for levels of a negative correlation energy centre relative to the valence band (E_V) and the conduction band (E_C) edges [34] (a), band diagram (b) and density-of-states distribution (c) for a reacted surface layer of PbS. The electron states between the mobility edges E_{Cm} and E_{Vm} are supposedly localized (see text for more detail).

by the level B^+ proceeds easier, producing the centre D^-, so the neutral defects D^0 with unpaired spins are unstable. A level C^+ may arise from the singly occupied centre in an excited configuration due to slow rearrangement of the rigid atomic network. An analogous set of states A^-, B^-, C^- takes place for transformations started from the negative defect. The centres D^+ and D^- usually are in equilibrium, and the Fermi level is pinned by the localized states in the middle of the gap [31–34].

In the reacted layers of galena, the mobility of normally octahedrally-coordinated S and Pb atoms is expected to be comparably low. As a consequence, defects D^+ and D^- may be not equilibrated and their concentrations may considerably differ [26]. The surfaces, which are passive in the anodic oxidation, appear to contain large amounts of donor-like centres exhibiting mainly the A^+-type levels (Figure 11(b)). This not merely decreases the density of holes but also gives rise to big potential fluctuations and so called Anderson localization of the states [31] in the upper part of the valence band (Figure 11(c)), sharply reducing the charge carrier mobility and the layer conductivity and so causing passivation. As a first approximation, there is no fundamental difference between disordered layers of various compositions, including those containing polysulfide species. However, if the depletion in metal is high and atoms are mobile enough, the defect conversion approaches the equilibrium, exhibiting B^+-type levels instead A^+ and preventing the passivation.

The charge associated with the gap states may be small, but it changes the character of surfaces and strongly affects some electrochemical reactions. According to Figure 11, the cathodic maximum C_1 corresponds to the recharging (in fact, reappearance) of the levels A^-. The C_2 and C_3 maxima were earlier ascribed to the reduction of 'easily reducible' surface elemental sulfur and inactive bulk one, respectively, yielding hydrogen sulfide [2]. Later, the reduction of overstoichiometric sulfur in the metal-deficient layer was suggested [5, 12]. Based on the scheme in Figure 11, the maximum C_2 at about -0.2 V may be connected with rather fast conversion of the centres represented by the B^+/B^- levels via the reorganization of metal–sulfur bonds in the vicinity of cation vacancies or the rupture of covalent S–S bonds in the elastic lattice

$$S + 2e^- \rightarrow S^{2-}, \quad (S-S)_n^{2-} + (2n-2)e^- \rightarrow nS^{2-} \qquad (5)$$

The 'active' monosulfide species S^{2-} bearing more negative charge than sulfide anions in intrinsic metal sulfides are thought to be the only centres which can specifically interact with hydrogen ions

$$S^{2-} + 2H^+ \rightarrow H_2S \qquad (6)$$

Such reactions of the excessive sulfur were proved to occur at pyrrhotite at the same potentials [47]. The peak C_2 shifts to more negative potentials after a pause between the anodic polarization and the negative-going potential excursion [2, 13] due to the formation of more 'rigid' atomic environment via the partial chemical dissolution of this 'active' sulfur (Equations 5 and 6) or/and the delivery of lead from the PbS bulk. The next cathodic feature C_3 corresponds to the transformation of A^+-type centres coupled with Reaction 6 and/or the electrodeposition of lead at 'rigid' spatial regions (Reaction 4). The bulk metallic Pb^0 and the metal deposited on various PbS sites with prevailing A^+, B^+, B^-, C^+ states oxidize at different potentials, showing the peaks A_3, A_4 and A_5. More research using methods of local characterization of the reacted surfaces is required to understand better these processes.

The dissolution of PbS is believed to proceed, akin to metal corrosion [48], via adsorption of acid anions which form, in competition with H_2O, OH^- and other ligands, surface lead complexes. Both the electrode potential and the anionic composition of the electrolyte affect the surface layer properties by governing the metal release rate and, therefore, the Pb/S ratio. Small admixtures of SO_4^{2-} and Cl^- ions to nitric acid solutions probably decrease the metal deficit, impeding atomic rearrangements within the reacted layers and PbS oxidation as a whole, and promoting Pb^{2+}/Pb^0 reactions.

5. Conclusions

This study demonstrates the correlation between the anodic behaviour and changes in surface topography and composition of lead sulfide. The surfaces, which are inactive in the anodic oxidation, are shown to facilitate the Pb^{2+}/Pb^0 redox transformation at negative biases. The approach developed as an alternative to the traditional explanations is based on the natural assumption that the disordered reaction layer of the semiconductor should be considered similarly to noncrystalline chalcogenides, the special characteristics of those are largely associated with two-electron negative correlation energy centres. The predominant donor-like defects formed in rather rigid structure of the reacted layer are supposed to limit the density of holes and to reduce the carrier mobility, thus depressing PbS oxidation and promoting metallic lead deposition in the course of potential cycling.

Acknowledgements

The authors are grateful to Russian Foundation for Basic Research (grant 01-03-32687a), and Krasnoyarsk Territory Science Foundation (grant 9F90) for financial support.

References

1. R.L. Paul, M.J. Nicol, J.W. Diggle and A.P. Saunders, *Electrochim. Acta* **23** (1978) 625.

2. R.L. Paul, M.J. Nicol, J.W. Diggle and A.P. Saunders, *Electrochim. Acta* **23** (1978) 635.
3. B. Dandapani and E. Ghali, *J. Electrochem. Soc.* **129** (1982) 271.
4. P. Sivenas and F.R. Foulkes, *Electrochim. Acta* **29** (1984) 1215.
5. Yu.L. Mikhlin, P.S. Galkin and N.A. Kopteva, *Izv. SO AN SSSR. Ser. khim. nauki* **7** (1988) 11.
6. E. Ahlberg and J. Ásbjornsson, *Hydrometallurgy* **34** (1993) 171.
7. P.R. Holmes and F.K. Crundwell, *Hydrometallurgy* **39** (1995) 353.
8. I. Cisneros-Gonzalez, M.T. Oropeza-Guzman and I. Gonzalez, *Hydrometallurgy* **53** (1999) 133.
9. I. Cisneros-Gonzalez, M.T. Oropeza-Guzman and I. Gonzalez, *Electrochim. Acta* **45** (2000) 2729.
10. J.L. Nava, M.T. Oropeza and I. González, *Electrochim. Acta* **47** (2002) 1513.
11. A.J. Parker, R.L. Paul and G.P. Power, *J. Electroanal. Chem.* **118** (1981) 305.
12. A.N. Buckley, I.C. Hamilton and R. Woods, *in* E. Fossberg (Ed.), 'Flotation of Sulphide Minerals' (Elsevier, Amsterdam, 1985), p. 41.
13. A.N. Buckley and R. Woods, *J. Appl. Electrochem.* **26** (1996) 899.
14. G.L. Pashkov, E.V. Mikhlina, A.G. Kholmogorov and Yu.L. Mikhlin, *Hydrometallurgy* **63** (2002) 171.
15. I.N. Plaksin and R.Sh. Shafeev, *Trans. Inst. Min. Metal.* **72** (1963) 715.
16. E.H.C. Parker and D. Williams, *Thin Solid Films* **35** (1976) 373.
17. P.E. Richardson and C.S. O'Dell, *J. Electrochem. Soc.* **132** (1985) 1350.
18. A.N. Buckley and R. Woods, *Appl. Surf. Sci.* **17** (1984) 401.
19. Yu.L. Mikhlin, A.V. Pashis and G.L. Pashkov, *Izv. SO AN SSSR. Ser. khim. nauki* **8** (1986) 123.
20. D. Fornasiero, F.S. Li, J. Ralston and R.St.C. Smart, *J. Colloid Interface Sci.* **164** (1994) 333.
21. C.A. Prestige, W.M. Skinner, J. Ralston and R.St.C. Smart, *Colloids Surf. A* **105** (1995) 325.
22. G. Wittstock, I. Kartio, D. Hirsch, S. Kunze and R. Szargan, *Langmuir* **12** (1996) 5709.
23. I. Kartio, K. Laajalehto, T. Kaurila and E.J. Suoninen, *Appl. Surf. Sci.* **93** (1996) 167.
24. I.V. Chernyshova and S.I. Andreev, *Appl. Surf. Sci.* **108** (1997) 225.
25. I. Kartio, K. Laajalehto, E.J. Suoninen, A.N. Buckley and R. Woods, *Colloids Surf. A* **133** (1998) 303.
26. Yu.L. Mikhlin, Ye.V. Tomashevich, I.P. Asanov and A.V. Okotrub, *Poverkhnost. Rentgen. Neitron. Synhrotron. Issled.* **12** (1998) 77.
27. R.St.C. Smart, W.M. Skinner and A.R. Gerson, *Surf. Interface Anal.* **28** (1999) 101.
28. Yu. Mikhlin, Ye. Tomashevich, I. Asanov and A. Okotrub, *in* R. Woods and F.M. Doyle (Eds), 'Electrochemistry in Mineral and Metal Processing V' (The Electrochemical Society Proceeding Series, Pennington, NJ, 2000), p. 282.
29. P. Novak and K. Laajalehto, *Appl. Surf. Sci.* **157** (2000) 101.
30. P. Novak, K. Laajalehto and I. Kartio, *Colloids Surf. A* **161** (2000) 447.
31. N.F. Mott and E.A. Davis, 'Electron Processes in Non-crystalline Materials' (Clarendon Press, Oxford, 1979).
32. M. Kastner, D. Adler and H. Fritzsche, *Phys. Rev. Lett.* **37** (1976) 1504.
33. M. Kastner and H. Fritzsche, *Phil. Mag.* **37** (1978) 199.
34. K.D. Tsendin (Ed.), 'Electron Phenomena in Chalcogenide Glassy Semiconductors', (Nauka, St. Peterburg, 1996).
35. C.M. Eggleston and M.F. Hochella, Jr., *in* 'Environmental Geochemistry of Sulfide Oxidation' ACS Symposium Series 550 (1994), p. 201.
36. U. Becker and M.F. Hochella, Jr., *Geochim. Cosmochim. Acta* **60** (1996) 2413.
37. C.M. Eggleston, *Geochim. Cosmochim. Acta* **61** (1997) 657.
38. B.S. Kim, R.A. Hayes, C.A. Prestige, J. Ralston and R.St.C. Smart, *Langmuir* **11** (1995) 2554.
39. S.R. Higgins and R.J. Hamers, *Surf. Sci.* **324** (1995) 263.
40. G. De Giudici and P. Zuddas, *Geochim. Cosmochim. Acta* **65** (2001) 1381.
41. D. Briggs and M.P. Seach, 'Practical Surface Analysis by Auger and X-ray Photoelectron Spectroscopy' (Wiley, Chichester and New York, 1983).
42. P.D. Scott and M.J. Nicol, *in* J.O'M Bockris, D.A.J. Rand, B.J. Welsh (Eds), 'Trends in Electrochemistry' (Plenum, New York and London, 1977) p. 303.
43. X. Zeng and S. Bruckenstein, *J. Electrochem. Soc.* **146** (1999) 2549.
44. N.P. Osipovich and E.A. Streltsov, *Russian J. Electrochem.* **36** (2000) 1.
45. K. Sangval, 'Etching of Crystals. Theory, Experiment, and Application' (North-Holland, Amsterdam, 1987).
46. D.J. Droppert and Y. Shang, *Hydrometallurgy* **39** (1995) 169.
47. Yu.L. Mikhlin, *Phys. Chem. Chem. Phys.* **2** (2000) 5672.
48. G.M. Florianovich and R.M. Lazorenko-Manevich, *Electrochim. Acta* **42** (1997) 879.